



# Evaluation of the Addition of Polypropylene (PP) Fibers in Self-compacting Concrete (SCC) to Control Cracking and Plastic Shrinkage Between Different Methods

**Jonatha Roberto Pereira<sup>a</sup>, João Batista Lamari Palma e Silva<sup>a\*</sup> , Luisa Andréia Gacher<sup>a</sup> ,**  
**Antonio Carlos dos Santos<sup>b</sup>, Rosa Cristina Cecche Lintz<sup>a</sup>**

<sup>a</sup>Universidade Estadual de Campinas (UNICAMP), Faculdade de Tecnologia, Limeira, SP, Brasil.

<sup>b</sup>Universidade Federal de Uberlândia, Departamento de Engenharia Civil, Uberlândia, MG, Brasil.

Received: December 15, 2022; Revised: May 13, 2023; Accepted: June 19, 2023

The present work aims to contribute to the study and development of methodologies for shrinkage tests of self-compacting concrete (SCC) using the addition of polypropylene (PP) microfibers as a variable to validate the correlations between the shrinkage tests. The objective of this work was to evaluate, through correlations between the area and the age at which the cracks appeared, the role of PP fibers as a control for this pathology. Reference SCC traces with additions of 6 mm and 12 mm microfibers were created for this purpose. For the shrinkage tests, the criteria of the ASTM C1579:2013 (plates) and ASTM C1581:2016 (rings) standards were used. The microfibers showed a significant reduction in cracks in the SCC, its reduction rate ranging from 40% to 70%, also presenting a delay in its appearance, which varied from 9 to 20 days for the appearance of the first crack.

**Keywords:** *self-compacting concrete, polypropylene fibers, concrete shrinkage, cracks.*

## 1. Introduction

An area as comprehensive and complex as civil engineering has a multitude of materials and composites that, with appropriate criteria, go far beyond what is expected in relation to their benefits and types of use. Concrete is one of these composite materials, and its high versatility, ease of production, and obtaining the raw material, as well as its specific properties and characteristics of production, molding, and curing, allow for the identification of variables that impair its behavior and make it susceptible to the appearance of pathologies or external agent attacks. Shrinkage, in its various types, is one of the properties resulting from the characteristics of concrete and internal processes generated during hardening<sup>1,2,3</sup>.

Shrinkage is an intrinsic phenomenon of cementitious composites and can be one of the following types: plastic shrinkage, drying shrinkage, chemical shrinkage, autogenous shrinkage, and thermal shrinkage<sup>4</sup>, which makes its study complex.

The shrinkage is the volume reduction caused by the loss of moisture in a concrete element, either in the fresh state or in the hardened state. In reinforced concrete, these volumetric changes of the paste are restricted by the presence of the large aggregate, the reinforcement or the form of the structural part. As the concrete is in the healing and increasing resistance phase, it is still not able to withstand the tensile stresses that arise superficially, which may come to generate cracks that can expand over time<sup>1</sup>.

In view of the concerns about controlling the appearance and opening of these cracks in concrete, the need for polymer fibers arises. These fibers are used to reduce segregation and shrinkage to drying or to increase fire resistance<sup>5</sup>.

The use of fibers and microfibers to reinforce concrete allows for increased stabilization of stresses generated during crack opening and material elasticity<sup>6</sup>. Therefore, the fibers have the characteristic of acting as a bridge for the transfer of surface stresses generated during the curing of concrete, reducing the existing tension and, consequently, the size of the opening of these cracks. Furthermore, the formation of cracks in concrete promotes the opening of the material's internal environment, which increases permeability and allows agents to degrade the internal structure of the concrete, compromising the durability of the projected part<sup>6</sup>.

One of the main factors related to cracking and shrinkage processes is the Portland cement hydration phenomenon. Studies and research aimed at understanding the chemical reactions that occur in this phase of hydration have been growing in recent years<sup>7</sup>.

The cement hydration process results from surface reactions between water and cement grain by means of dissolution-precipitation mechanisms or topochemical reactions (hydration in the solid state), which release heat (exothermic), raising the temperature. This temperature increase in turn, requires a greater guarantee of hydration of the cement grain, and, when this does not occur, the hardening process of the cement can be compromised, causing, in many cases, the retraction of the piece<sup>7,8,9</sup>.

\*e-mail: lamaripalma@hotmail.com

According to Pons and Torrenti<sup>9</sup>, the profile of current structures requires, in many cases, a high consumption of cement, higher characteristic resistances, restriction to heat dissipation and that may have a lower dilation and shrinkage value, such as so-called special concrete, such as high-performance concrete (HPC) and self-compacting concrete (SCC).

Over the years, numerous studies have been developed in order to better understand the behavior of SCC<sup>2,10,11</sup> and considerations presented by Campos<sup>12</sup> and Miranda et al.<sup>13</sup>, highlight the importance of improving its properties, study new additions in its composition and verify its applicability and behavior in structural parts.

To obtain a SCC, higher amounts of fines, the use of superplasticizers, a lower consumption of large aggregates, a water/cement ratio of approximately 0.4 and aggregates of good shape and texture are used<sup>14,15</sup>. However, these characteristics may cause the SCC to crack more due to shrinkage caused by drying or plastic shrinkage, which may compromise its durability. Thus, the addition of fibers to concrete aims to have a direct effect on the gains in cracking strength, bending strength, and contributing to the prevention of SCC retraction.

Controlling concrete cracking is critical for increased elements durability over time and the development of strength in the early stages<sup>6,16</sup>. The justification is that the cracks generated create critical points, in which there is an increase in the surface sensitivity of the concrete, making it susceptible to external attacks that damage the concrete rebar. In this way, the performance, the need for maintenance, the durability of the elements and aesthetics of the structures and concrete are also reduced.

The use of fibers, such as polypropylene (PP) in the production of concrete, usually collaborates with the improvement of their mechanical properties<sup>17</sup>. Several studies have evaluated the properties of concretes with PP fibers, especially the properties in the hardened state, leaving aside in many cases the harmful effects caused by workability<sup>18</sup>. In the same sense, Aslani et al.<sup>19</sup>, point out that given the positive and negative effects of adding PP fibers to concrete, its effects should always be previously considered for use in structures.

This reduction in the workability of concrete with fibers varies according to the different properties, such as: type of fiber, geometry of fiber, aspect ratio, and volume<sup>20</sup>. However, studies<sup>21</sup> show that the combination of other materials (as silica fume) and the use of superplasticizers in the production of SCC with PP fiber can contribute to the improvement of properties with good flowability, viscosity, and passing ability.

The present work aims to contribute to the study and development of methodologies for SCC retraction tests using the addition of PP microfibers as a variable for the validation of correlation retraction tests, and the crack area and age of the emergence of SCC cracks.

Recent research<sup>22,23,24</sup> follow the ASTM C1579:2013 (plates) and ASTM C1581:2016 (rings) standards for the evaluation of shrinkage and cracking in concrete in a different way, however, this research employs the use of both standards to evaluate the properties of SCC with PP fiber.

## 2. Experimental Materials and Methods

### 2.1. Materials

#### 2.1.1. Cement

Type of cement used was CPV-ARI, with specific gravity of 3.15 kg/dm<sup>3</sup>. This type of cement was chosen due to its fineness modulus, which is smaller than that of other cements provided in ABNT NBR 16697<sup>25</sup> and contributes to the production of SCC.

#### 2.1.2. Aggregate

The sand used presented a specific gravity of 2.65 kg/dm<sup>3</sup> and unit mass in the loose and dry state of 1.52 kg/dm<sup>3</sup>. The aggregate used for the production of concrete is basaltic. It presented a specific gravity of 2.90 kg/dm<sup>3</sup> and a compact unit mass of 1.51 kg/dm<sup>3</sup>. The gravel powder used presented a specific gravity of 2.64 kg/dm<sup>3</sup> and unit mass in the loose and dry state of 1.58 kg/dm<sup>3</sup>. In relation to the microfibers, polypropylene polymer fibers were used, with a length of 6 and 12 mm, with a diameter of 21 µm, specific gravity 0.91 g/cm<sup>3</sup> and elasticity modulus of 3.0 GPa, as shown in Figure 1.

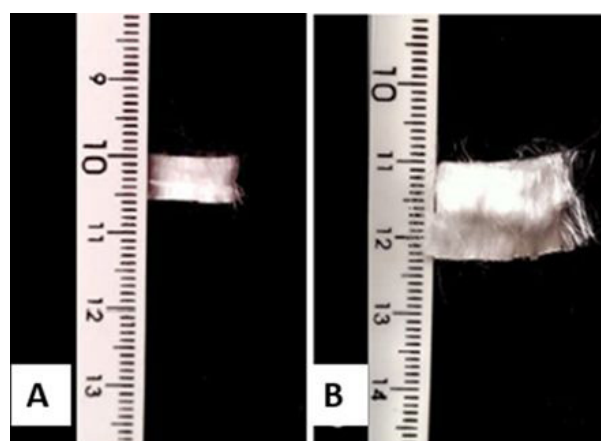


Figure 1. 6 mm fibers (A); 12 mm fibers (B).

### 2.1.3. Superplasticizer

The additive used is the base of polycarboxylate ether and has the ability to increase the workability of the mixture, keeping the properties of the material intact, such as its homogeneity. It has a density of 1.09 g/cm<sup>3</sup>.

### 2.1.4. Mix proportions

The mix for both lengths (6 and 12 mm) of PP fiber followed the proportions indicated in Table 1.

## 2.2. Methods

### 2.2.1. Vials for the testing of plates used in the evaluation of plastic shrinkage

For the execution of the plate tests, two dimensions of plates were established, one in the dimension of 560 x 350 x 50 mm<sup>3</sup> (length x width x height) as set out in ASTM C1579<sup>26</sup> and another square plate proposed in this work in the dimension of 300 x 300 x 50 mm<sup>3</sup> (length x width x height).

All plates were produced in metallic material in order to retain maximum water in the cement hydration process. As shown in Figure 2, the formwork was produced with three fixed sides and one removable side to facilitate the disshaping of the piece. Metal parts with an internally positioned "U" section of 25 x 35 x 75 mm<sup>3</sup> were fixed inside the formwork for internal restriction effect with 50 mm spacing of the shape face.

### 2.2.2. Vials for the ring test used in the evaluation of SCC retraction and the age of crack appearance

It was elaborated rings, following exactly the parameters of the standard<sup>27</sup> as presented in Figure 3. The base was made of reinforced wood and acrylic coating to avoid absorption of the hydration water in the drying process and avoid the adherence so as not to harm the test.

The cracking happens in this test, as a result of drying and autogenous shrinkage, as well as the heat of hydration of the cement<sup>28</sup>.

**Table 1.** Traces in the proportion of cement mass.

Cement	PP fiber (%)	Sand	Gravel powder	Gravel	Superplasticizer (%)	w/c
1	0	1.45	1.28	1.05	1	0.65
1	0.05	1.45	1.28	1.05	1	0.65
1	0.10	1.45	1.28	1.05	1	0.65

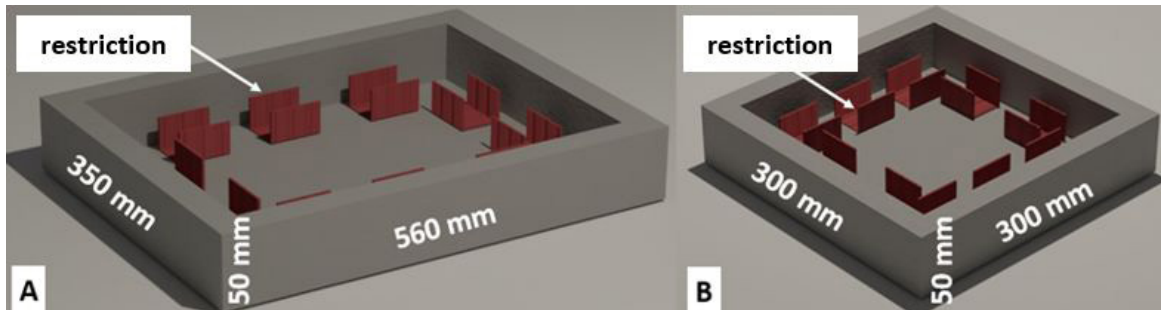


**Figure 2.** (A) Rectangular plate for the testing of cracks; (B) Square plate for crack testing.

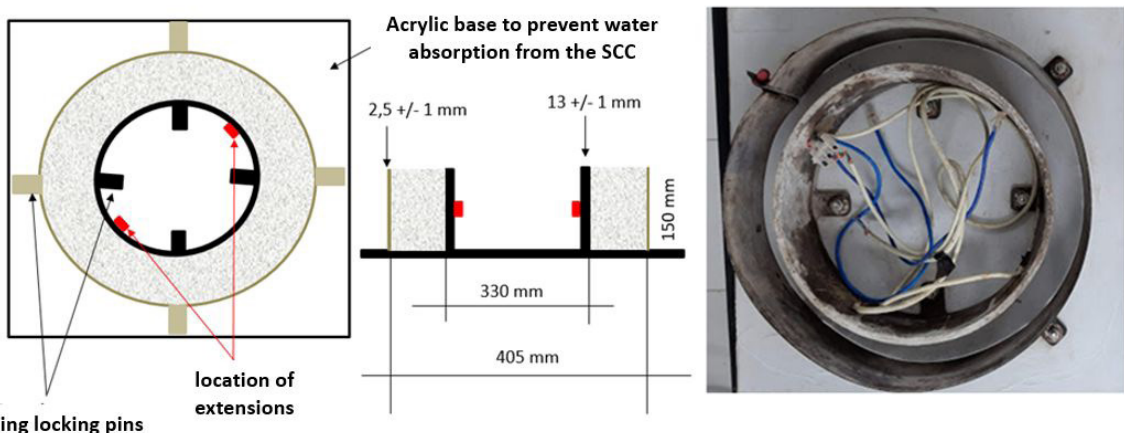


**Figure 3.** Mold for ring testing according to the dimensions of ASTM C1581:2016<sup>27</sup>.

### 2.2.3. Molding and testing of plates

For the molding and testing of the plates, the specifications of ASTM C1579<sup>26</sup> and ACI 305R-91<sup>29</sup> were followed. First, criteria were established for temperature, wind speed and relative humidity, which establishes an evaporation rate above  $0.51 \text{ kg/m}^2/\text{h}$  for the probability of cracking in concrete parts. For the respective test, an average temperature of  $36 \pm 1^\circ\text{C}$ ,  $46 \pm 1\%$  was established for relative humidity (RH) and constant wind speed of  $2.5 \pm 1 \text{ m/s}$ , measured five centimeters above the plate during all tests performed. For wind speed measurement, a digital wind measurement anemometer was used. Because it is a SCC, a fixed point of release of the mixture was established, until the SCC fills the form by complete.

Then, the concrete plates were placed inside the control chamber, thus initiating the cracking tests. Figure 4 presents the methodology of the cracking test according to the criteria of the standard<sup>26</sup>.

After the 24-hour period of the test, the plates were removed from the control chamber and then the cracks were mapping by calculating the average width and length. For this, a digital caliper, magnifying glass was used to facilitate the identification and the crack ruler.

The results were transformed into medium areas of cracking and then in reduction rate.

### 2.2.4. Molding for the ring test

In relation to the test of the restriction ring, the criteria of the standard were established<sup>27</sup>. With the data acquisition system (DAQ) configured and validated, the SCC rings were molded. Then, after molding, the temperature of the SCC was checked using a laser thermometer to establish the variation of the information and maintain the same criteria in all trials. An environment with an average temperature of  $30 \pm 1^\circ\text{C}$  and relative humidity of  $62 \pm 1\%$  was established.

The molding started and remained at a fixed point of the ring and because it is SCC there was no manual densification and no need for variation of the launch point. The measurements of the strain gauges ( $\mu\text{m}/\text{m}$ , ring's strain) were programmed to measure one time per minute. According to the standard<sup>27</sup> a sudden decrease in strain in  $\mu\text{m}$  or both strain gauges indicate the probability of the appearance of cracks.

The set has been placed in a fixed place to avoid any kind of variation. A digital thermometer performed the measurement of air temperature and humidity at the time of the test as shown in Figure 5.

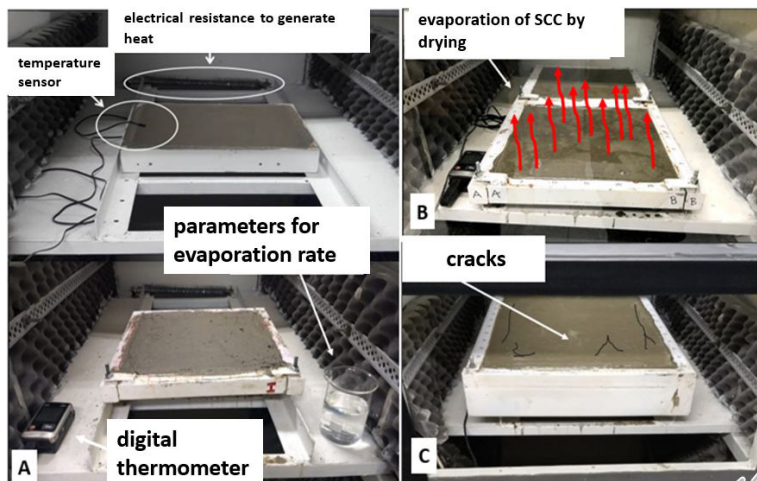


**Figure 4.** (A) Identification of measurement sensors and fin resistance for internal heat generation; (B) Evaporation of water to speed up the drying process; (C) Appearance of cracks.

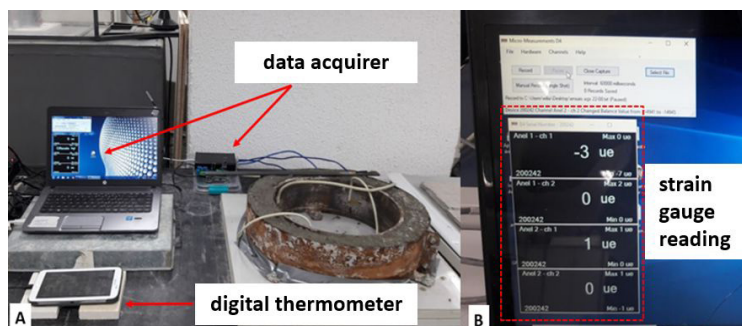


**Figure 5.** Methodology for the test of the ring with restriction: A - Installation set for retraction test and crack age; B - Strain reading template measured by strain gauges.

### 3. Results and Discussion

#### 3.1. SCC-restricted plates

By means of the width of the cracks and the measurement of their length, it is possible to calculate the average cracking area of the SCC plates. Table 2 presents the respective results of the mean of the cracking areas.

The  $\text{SCCRF}_0$  presented an average cracking area of  $1,201.30 \text{ mm}^2$  for plate  $350 \times 560 \text{ mm}$  and  $375.05 \text{ mm}^2$  for the plate with  $300 \times 300 \text{ mm}$ . With the addition of fibers throughout the tests it was possible to observe a reduction in the cracking area and in the average width of the cracks.

Another factor that directly influenced these reductions was the length of the fibers. The  $\text{SCCRF}_6 - 6 \text{ mm}$  trait presented a reduction rate in the mean area of cracks ranging from 47.35% to 51.72%. In the case of  $\text{SCCRF}_{12} - 12 \text{ mm}$  traces there was a variation between 67.87% and 70.95%.

According to Cristofoli et al.<sup>30</sup>, Alferes et al.<sup>31</sup>, and Monte et al.<sup>32</sup> the content and length of the fibers act as a bridge of stress transfers, that is, the higher the fiber content, the lower the emergence or development of cracks, whether for synthetic fibers or metal fibers.

According to Ali et al.<sup>20</sup> the reduction of areas of SCC cracks are linked to reduction of the widths of the cracks due to the effect of the "seam" of the particles of the concrete surface that can reach up to 55% of the reduction.

#### 3.2. Ring with SCC restriction

According to the results presented it is possible to verify that all traces have a similar characteristic. They have a period of compression of the ring, a point of fall in the strain and then a relaxation of this stress.

For the elaboration of the graphs and in order to facilitate the interpretation of the data, the mean strains ( $\mu\text{m}/\text{m}$ ) per day were used by reading the strain gauges.

Figure 6 presents the results of the tests of the restriction ring with the addition of the 6 mm fibers and according to the criteria established by the standard<sup>27</sup>.

**Table 2.** Crack area and SCC reduction rate.

Fibers	Cracking area ( $\text{mm}^2$ )			Fibers	Cracking area ( $\text{mm}^2$ )			
	BOARD 350 X 560 mm				BOARD 300 X 300 mm			
	0%	0.05%	0.10%		0%	0.05%	0.10%	
$\text{SCCRF}_0$	1,201.30	-	-	$\text{SCCRF}_0$	375.03	-	-	
$\text{SCCRF}_6 - 6 \text{ mm}$	-	632.50	579.98	$\text{SCCRF}_6 - 6 \text{ mm}$	-	222.00	207.60	
$\text{SCCRF}_{12} - 12 \text{ mm}$	-	386	349	$\text{SCCRF}_{12} - 12 \text{ mm}$	-	70.65	52.28	
Crack Area Reduction Rate ( $\text{mm}^2$ )								
Fibers	BOARD 350 X 560 mm			Fibers	BOARD 300 X 300 mm			
	0%	0.05%	0.10%		0%	0.05%	0.10%	
$\text{SCCRF}_0$	-	-	-	$\text{SCCRF}_0$	-	-	-	
$\text{SCCRF}_6 - 6 \text{ mm}$	-	47.35%	51.72%	$\text{SCCRF}_6 - 6 \text{ mm}$	-	40.80%	44.64%	
$\text{SCCRF}_{12} - 12 \text{ mm}$	-	67.87%	70.95%	$\text{SCCRF}_{12} - 12 \text{ mm}$	-	81.16%	86.06%	

It is possible to verify that until the 13<sup>th</sup> day the  $\text{SCC}_{\text{RFtraces}}$  presented a pattern of ring strain in relation to time. However, between the 14<sup>th</sup> day and the 19<sup>th</sup> day the traces begin to present the individual differences referring to each trait performed. In relation to the  $\text{SCCRF}_{0\text{trace}}$ , the strain variation can be verified between the 9<sup>th</sup> and 10<sup>th</sup> day, i.e., the sudden change in strain corresponds to the age of cracking visible in the sample.

Regarding the  $\text{SCCRF}_{6 - 6\text{mm}}$  -0.05% trace, the variation of the strain was verified on the 12<sup>th</sup> and 13<sup>th</sup> day of the beginning of the ring test, a difference of approximately 3 days when compared to  $\text{SCC}_{\text{RF}0}$ . The crack spawn points did not present a specific location; in each trace it was possible to verify the appearance of the cracks in different places of the ring. The average widths of the cracks vary between 0.30 and 0.40 mm.

The  $\text{SCCRF}_{12 - 12\text{mm}}$  trace presented an average age of crack approximately 17.5 days after the beginning of the test as shown in Figure 7.

Regarding ring strain it was verified that for the points predicted for cracking age the strain ranged from -35 to -45  $\mu\text{m}/\text{m}$ . The cracks did not present an opening pattern the width crack was 0.20 to 0.30 mm.

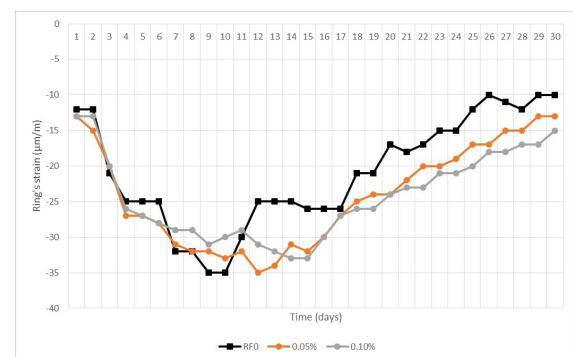


**Figure 6.** Graph of the strain *versus* age of cleft  $\text{SCC}_{\text{RF}6\text{mm}}$  according to the criteria established by the ASTM C1581:2016<sup>27</sup> standard.

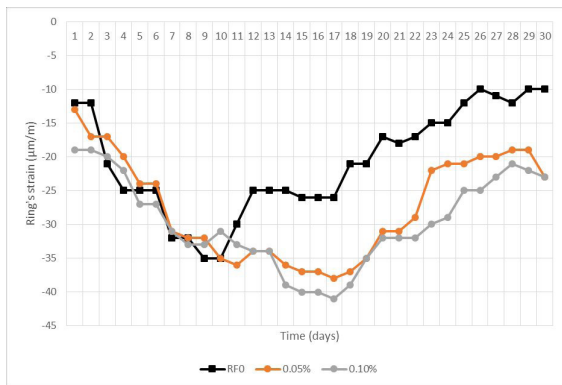


**Figure 7.** Graph of strain *versus* age of cleft SCCRF<sub>12mm</sub> according to the proposal of ring reduction with an alternative for SCC tests.

Other authors also obtained results similar to this research<sup>33</sup> evaluated the retraction by drying according to ASTM C1581/C1581M<sup>27</sup>, of concretes with different types of fibers: 0.25% and 0.5% of vegetable fibers (sisal and rami) and 0.25% of polypropylene fiber. According to the results found, ring strain varied from 0 to -80  $\mu\text{m}/\text{m}$ .

A study<sup>34</sup> evaluated the performance of concrete with different fibers in terms of shrinkage. The maximum strain of 30 in the ring test checked for the concrete with polypropylene fibers. The appearance of the crack occurred at 66 hours of testing.

Another study<sup>35</sup> showed when varying the content of addition of micro silica and fly ash in the composition of the SCC observed that the age of cracking occurred between the 4<sup>th</sup> and 10<sup>th</sup> day with a strain of the ASTM ring, ranging from 10 in the expansion phase to -80  $\mu\text{m}/\text{m}$  in the compression phase.

Researchers<sup>36,37</sup> measured by means of the ring test, the retraction of high strength concrete with the addition of polypropylene fibers. For the test, reference traces were performed with the addition of 0.3; 0.6 and 0.9% polypropylene fibers in relation to the volume of concrete. The trace without addition of fibers presented the first crack in the 10. In relation to the traces with the addition of fibers, the authors observed a gain in the appearance of the first cracks. Ring strain ranged from -20 to -90  $\mu\text{m}/\text{m}$ .

## 4. Conclusions

The main goal of this research was to analyze the correlation of the SCC retraction tests with the addition of PP microfibers as comparison variables. Through the proposed methodology and the results found, it is concluded that:

SCC characteristics such as additive consumption, higher mortar content, and reduction of coarse aggregate, combined with variables such as shape area, temperature, evaporation rate, drying speed, and relative humidity, were determining factors for the appearance of cracks.

The formwork reduction proposal presented similar results to the models presented by the ASTM C1579:2013 standard, allowing them to be used as alternatives for SCC retraction studies, mainly in studies with the addition of fibers in lengths of 6 and 12 mm.

The fibers influenced the reduction of crack areas and delayed their appearance. The fibers with the highest content and those with the greatest length showed the best results in reducing the appearance of cracks. However, they also caused a loss of scattering in the fresh SCC state.

The PP microfibers influenced the workability and viscosity of the SCC in its fresh state. However, the sewing effect of the microfibers showed a direct correlation with the rate of reduction of widths and crack areas in the SCC.

Regarding the correlations, it is concluded that the shape area directly influenced the cracking area in the SCC. The crack width did not have a direct influence on the cracking area.

In the restricted ring test, according to the ASTM criteria, the length of the fibers presented the best correlation. This fact can be analyzed due to the methodology of the expansion and contraction tests. Fibers with greater lengths allowed a greater extension in the load transmission bridge, thus delaying the appearance of cracks.

The results found demonstrate the need to establish methods and criteria for shrinkage tests and the understanding of the formation of cracks in the SCC, considering the variables that influence the mixing, launching, and drying of the concrete specimens. Understanding the correlations between these variables contributes to reducing the appearance of cracks and, consequently, to greater durability and quality of concrete specimens, minimizing future issues.

## 5. Acknowledgements

The authors acknowledge the financial support provided by: CAPES (Coordination for the Improvement of Higher Education Personnel, Ministry of Education, Brazil) – Financing Code 001 - Jonatha Roberto Pereira. CNPq (National Council for Scientific and Technological Development, Ministry of Science, Technology, Innovation and Communications, Brazil): Prof. Luís Andréia Gachet (310375/2020-7; 406234/2018-3), Prof. Rosa Cristina Cecche Lintz (PQ2, Process number: 310376/2020-3). FAPESP (São Paulo Research Foundation): Prof. Rosa Cristina Cecche Lintz (2018/12076-5), Prof. Luís Andréia Gachet (2018/14945-0).

## 6. References

1. Soares RV. Study of the strength resulting from shrinkage and temperature variation in reinforced concrete structures. Rio de Janeiro: Department of Civil Engineering/PUC; 2015. In Portuguese.
2. Alcântara MAM, Granju J-L, Pons G, Mouret M. Comparative study of mono and bi-fiber solutions for cases of self-compacting concrete and glazed concrete. In: 1st National Meeting of Research, Design and Production of Precast Concrete; 2005 Nov 3-4; São Carlos. Proceedings. São Carlos: EESC/USP; 2005. p. 1. In Portuguese.
3. Barbosa M, Carvalho C, Delfino RR, Alves JA, Andrade EFO, Dantas MP. Production of high performance concrete (HPC) with the addition of stone powder. InterScientia. 2019;7(1):200-17.
4. Vianna NJ, Forti NCS, Moraes GP, Silva JBLP. Drying shrinkage of fiber reinforced concrete under restrained conditions: a systematic mapping study. In: Iano Y, Saotome O, Vásquez GLK, Pezzuto CC, Arthur R, Oliveira GG, editors. Proceedings of the 7th Brazilian Technology Symposium (BTSym'21). Emerging trends in systems engineering mathematics and physical sciences. Vol. 2. Cham: Springer; 2022. p. 84-94. Smart Innovation, Systems and Technologies, vol. 295.

5. EFNARC: European Federation of Specialist Construction Chemicals and Concrete Systems. The European guidelines for self-compacting concrete. Surrey: EFNARC; 2010.
6. Kakoeei S, Akil HM, Jamshidi M, Rouhi J. The effects of polypropylene fibers on the properties of reinforced concrete structures. *Constr Build Mater.* 2012;27(1):73-7.
7. Gambale PG. Study of the heat of hydration of concrete mass and contribution to thermal calculation and prediction of retraction cracks [dissertation]. Goiânia: Federal University of Goiás; 2017. In Portuguese.
8. Nam J, Kim G, Yoo J, Choe G, Kim H, Choi H et al. Effectiveness of fiber reinforcement on the mechanical properties and shrinkage cracking of recycled fine aggregate concrete. *Materials.* 2016;9(3):131.
9. Pons G, Torrenti JM. Shrinkage and flow. In: Olliver J-P, Vichot A, editors. *Concrete durability - scientific bases for the formulation of durable concrete according to the environment.* São Paulo: IBRACON; 2014. p. 139-80. In Portuguese.
10. Angelin AF, Silva FM, Giorno LS, Lintz RCC, Barbosa LAG. Physical and mechanical properties of self-compacting concrete modified with expanded clay and rubber powder. In: 57th Brazilian Concrete Congress; 2015 Oct 27-30; Bonito. Proceedings. São Paulo: IBRACON; 2015. p. 1-15. In Portuguese.
11. Long WL, Khayat KH, Lemieux G, Xing F, Wang WL. Factorial design approach in proportioning prestressed self-compacting concrete. *Materials.* 2015;8(3):1089-107.
12. Campos RS. Self-compacting concrete produced with construction and demolition waste: mechanical and rheological properties [dissertation]. Campinas: Pontifical Catholic University of Campinas; 2017. In Portuguese.
13. Miranda LRM, Morais GAT, Lira VQ, Abreu MM. Evaluation of compressive strength and performance against chloride corrosion of self-compacting concrete produced with the addition of biopolymer. In: National Conference on Pathology and Structures Recovery (CONPAR); 2017 Aug 30-31; Recife. Proceedings. Recife: Escola Politécnica de Pernambuco; 2017. p. 1-13. In Portuguese.
14. Kar S, Sanjay SS. Effect of admixtures on shrinkage properties in self-compacting concrete. *Int J Res Eng Technol.* 2016;5(2):292-6.
15. Jadhav SH, Pawar VV, Dokhale RR. A review report on plastic shrinkage of concrete & self-compacting concrete. *Int J Adv Eng Res Sci.* 2017;6(3):541-50.
16. Acker P, Torrenti JM, Guérinet M. Cracking control in the early ages: condition of durability of concrete works. In: Olliver J-P, Vichot A, editors. *Concrete durability - scientific bases for the formulation of durable concrete according to the environment.* São Paulo: IBRACON; 2014. p. 181-206. In Portuguese.
17. Aslani F, Gedeon R. Experimental investigation into the properties of self-compacting rubberised concrete incorporating polypropylene and steel fibers. *Struct Concr.* 2019;20(1):267-81.
18. Matar P, Assaad JJ. Concurrent effects of recycled aggregates and polypropylene fibers on workability and key strength properties of self-consolidating concrete. *Constr Build Mater.* 2019;199:492-500.
19. Aslani F, Hou L, Nejadi S, Sun J, Abbasi S. Experimental analysis of fiber-reinforced recycled aggregate self-compacting concrete using waste recycled concrete aggregates, polypropylene, and steel fibers. *Struct Concr.* 2019;20(5):1670-83.
20. Ali A, Hussain Z, Akbar M, Elahi A, Bhatti S, Imran M et al. Influence of marble powder and polypropylene fibers on the strength and durability properties of self-compacting concrete (SCC). *Adv Mater Sci Eng.* 2022;2022:9553382.
21. Liu X, Wu T, Yang X, Wei H. Properties of self-compacting lightweight concrete reinforced with steel and polypropylene fibers. *Constr Build Mater.* 2019;226:388-98.
22. Meyer DM, Combrinck R. Utilising micro CT scanning technology as a method for testing and analysing plastic shrinkage cracks in concrete. *Constr Build Mater.* 2022;317:125895.
23. Cai C, Tang H, Wen T, Li J, Chen Z, Li F et al. Long-term shrinkage performance and anti-cracking technology of concrete under dry-cold environment with large temperature differences. *Constr Build Mater.* 2022;349:128730.
24. Liu Y, Wei Y, Ma L, Wang L. Restrained shrinkage behavior of internally-cured UHPC using calcined bauxite aggregate in the ring test and UHPC-concrete composite slab. *Cement Concr Compos.* 2022;134:104805.
25. ABNT: Associação Brasileira de Normas Técnicas. ABNT NBR 16697: Portland Cement – requirements. São Paulo: ABNT; 2018. In Portuguese.
26. ASTM: American Society for Testing and Materials. ASTM C1579: standard test method for evaluating plastic shrinkage cracking of restrained fiber reinforced concrete (using a steel form insert). West Conshohocken: ASTM; 2013.
27. ASTM: American Society for Testing and Materials. ASTM C1581/C1581M: standard test method for determining age at cracking and induced tensile stress characteristics of mortar and concrete under restrained shrinkage. West Conshohocken: ASTM; 2016.
28. Vianna NJ, Moraes GP, Forti NCS, Silva JBLP, Jacintho AEPGA, Pimentel LL. Study of cracking due to restrained shrinkage on microfibers reinforced concretes. In: 63º Brazilian Concrete Congress; 2022 Oct 11-14; Brasilia. Proceedings. São Paulo: IBRACON; 2015. p. 1-14. In Portuguese.
29. ACI: American Concrete Institute. ACI 305R-91: guide to hot weather concreting. Farmington Hills: ACI; 2010.
30. Cristofoli T, Silva G, Tutikian B, Christ R. Influence of the addition of metallic fibers in self-compacting concrete in the hardened state. In: V Ibero-American Congress on Self-compacting Concrete and Special Concretes; 2018 Mar 5-6. Valencia. Proceedings. Valencia: Universitat Politècnica de València; 2018. p. 445-54.
31. Alferes R Fo, Monte R, Figueiredo AD. Evaluation of steel fiber orientation in slab elements induced during casting with self-compacting concrete. *Rev Matéria.* 2019;24(2):e12340.
32. Monte R, Barros MMSB, Figueiredo AD. Evaluation of early age cracking in rendering mortars with polypropylene fibers. *Ambient Constr.* 2018;18(2):21-32.
33. Borges APSN, Motta LAC, Pinto EB. Study of concrete properties with addition of plant fibers and polypropylene for use in structural walls. *Rev Matéria.* 2019;24(2):e12364.
34. Yang Y, Ma L, Huang J, Gu C, Xu Z, Liu J et al. Evaluation of the thermal and shrinkage stresses in restrained high-performance concrete. *Materials.* 2019;12:3680.
35. Altoubat S, Junaid MT, Leblouba M, Badran D. Effectiveness of fly ash on the restrained shrinkage cracking resistance of self-compacting concrete. *Cement Concr Compos.* 2017;79:9-20.
36. Sayahi F, Emborg M, Hedlund H. Effect of water-cement ratio on plastic shrinkage cracking in self-compacting concrete. In: 23th Symposium on Nordic Concrete Research & Development; 2017 Aug 21-23; Aalborg. Proceedings. Oslo: Norsk Betongforening; 2017. p. 339-42.
37. Zhou X, Dong W, Oladiran O. Experimental and numerical assessment of restrained shrinkage cracking of concrete using elliptical ring specimens. *J Mater Civ Eng.* 2014;26(11):04014087.